This is an author's version published in: http://oatao.univ-toulouse.fr/27483

Advances in the control of electrophoretic process parameters to tune the ytterbium disilicate coatings microstructure

Manon Prioux[1] (ID) | **Sandrine Duluard**[1] (ID) | **Florence Ansart**[1] | **Guillaume Pujol**[2]
Philippe Gomez[2] **Lisa Pin**[3]

[1]Université de Toulouse, CNRS, INPT, UPS, Université Toulouse 3Paul Sabatier, Bât CIRIMAT, Toulouse Cedex 9, France

[2]DGA Aeronautical Systems, Balma Cedex, France

[3]Safran Ceramics, Merignac, France

Correspondence

Manon Prioux, Université de Toulouse, CNRS, INPT, UPS, Université Toulouse 3 Paul Sabatier, Bât CIRIMAT, 118 Route de Narbonne, 31062 Toulouse Cedex 9, France.
Email: prioux@chimie.ups-tlse.fr

Funding information
Safran; DGA

Abstract

Suspensions of ytterbium disilicate in isopropanol were prepared using iodine dispersant. Their zeta potential, electrical conductivity, and pH dependence with iodine concentration is detailed. Electrophoretic deposition was performed on silicon substrates at various voltages (100-200 V) and times (until 10 minutes) and the growth dynamic was investigated. It was observed that the deposited mass reaches a maximum value for $[I_2] = 0.2$ g/L, and the coating microstructure becomes porous at higher iodine concentrations. Current density and voltage measurements allowed to correlate this behavior to the increase of free protons concentration in the suspension. In these conditions, it was proved that porosity increases with the increase in applied voltage, and a compaction occurs as the deposition time increases. This has been related to the coating resistance increase and subsequent decrease in effective voltage in the suspension. The denser coatings (20% of porosity) were obtained in the case of suspension without iodine, at the minimum applied voltage and for the longest deposition times.

KEYWORDS

coatings, electrophoretic deposition, environmental barrier coatings (EBC), microstructure

1 INTRODUCTION

Rare earths silicates find many applications in aeronautics or energy field. One of them is relative to the high temperature protection of ceramics such as SiC-based materials. Generally, environmental barrier coatings (EBCs) are needed to protect SiC-based ceramic materials against water vapor corrosion at high temperature.[1] The development of such coating systems is necessary to implement SiC/SiC ceramic matrix composites in hot section components of advanced gas turbine machine.[2] Indeed, at high temperature in dry air, the SiC/SiCs react with oxygen to form a thin protective silica layer. However, in combustion environment, water vapor reacts with the silica, forming gaseous reaction products such as $Si(OH)_4$, leading to severe recession of the SiC.[3-5] Ytterbium disilicate $Yb_2Si_2O_7$ is a promising material for

EBCs, because it has an excellent resistance to volatilization and a thermal expansion coefficient close to that of the SiC/SiC substrate one (5.06×10^{-6}/°C for SiC and 4.5×10^{-6}/°C for $Yb_2Si_2O_7$).[6] Moreover $Yb_2Si_2O_7$ exhibits a single phase structure up to about 1600°C.[7] The properties of EBCs vary with the different preparation processes. There are several methods to produce ceramic coatings, such as chemical vapor deposition, physical vapor deposition, ion implantation, thermal-spray, soft chemistry including sol-gel routes and newly developed electrophoretic deposition (EPD).[8-12]

Electrophoretic deposition is a suspension processing technique, and is increasingly gaining applications in manufacturing of thin and thick films, laminates, advanced functional coatings, porous materials, ceramics with complex geometric shape, or thermal barrier coatings.[13-15] Once the EPD processing and suspension parameters well were

determined, this process is robust, rapid, low-cost and versatile. EPD is a two steps process: (a) migration of charged particles in a suspension under an electric field between two electrodes, and (2) particles coagulation on one of the electrode surface.[16] The preparation of a stabilized parbticles suspension is essential to obtain homogeneous and reproductive coatings. The stability is achieved by adjusting inter-particles forces.[17-18] The optimization of the process parameters such as applied deposition voltage and time is necessary to tune the deposit microstructure (thickness, density, homogeneity). Suspension properties and stability depend on the nature (metallic, ceramic, or polymer), size, and concentration of the particles, type of solvent and additives. Most of the works in the EPD field correspond to non-aqueous media. Organic liquids and alcohols offer many advantages such as their good chemical stability, which avoid adverse reactions to the electrode, disrupting the formation of the coating.[16] Among the conventional solvents used in EPD, isopropanol is a good candidate due to its low dielectric constant (19.4), low viscosity (2.04 mPa s), and a moderate evaporation rate (saturated vapour pressure equal to 4.4 kPa).[19-21] The kinetics of EPD has also been widely investigated.[16,22-24] In particular, controlling the kinetics during EPD makes possible the control of the desired mass/thickness of deposit. In a first approximation, the Hamaker model for EPD kinetics is proposed:[25]

$$\frac{dw}{dt} = \mu \times c \times A \times E, \tag{1}$$

with dw/dt the deposition rate (g/s), μ the electrophoretic mobility of particle (cm^2/(s V)), c the particles concentration in the suspension (g/cm^3), A the deposition area (cm^2), and E the applied electric field (V/cm). The electrophoretic mobility μ is calculated using the following equation:[26]

$$\mu = \frac{\varepsilon_0 \varepsilon_r \xi}{n}, \tag{2}$$

with ε_0 the vacuum permittivity, ε_r the relative dielectric constant of the suspension medium, ξ the zeta potential of particles, and η the viscosity of the solvent. However, this model is only relevant for low concentrations and short experiments. In general, the evolution of the different parameters with time must be taken into account: depletion in particles concentration, evolution of suspension parameters (conductivity, etc…), decrease of the efficient voltage due to the electrically resistive character of the deposited coating, etc In ethanol-based suspensions, Sarkar and Nicholson suggested that the decrease of the deposited mass is mainly influenced by the decrease of both solid loading in the suspension and electric field.[22] Ferrari and Moreno took into account the change of the conductivity of alumina suspensions with time during EPD.[23] For ytterbium disilicates, such

systematic study of the kinetics is necessary to determine the deposited mass depending on the deposition parameters.

The aim of this present work was to investigate EPD of ytterbium disilicate ($Yb_2Si_2O_7$) coatings from suspension prepared with isopropanol and iodine (I_2) as conductivity modifier, and to study the effect of various parameters such as the iodine concentration, applied voltage and deposition time on the EPD kinetics and on the morphological properties of the $Yb_2Si_2O_7$ coatings.

2 | EXPERIMENTAL PROCEDURE

2.1 | Materials

Ytterbium disilicate powder (Marion Technologies France, 214.270.007) with an average particles size of 300 nm was used as received. Isopropanol (>99%; Merck) and Iodine I_2 (99.5%; Fisher chemical) were used as solvent and dispersant, respectively. Silicon wafers were used as substrates (Sil'tronix Silicon Technologies, France, stock list reference W3707, P-boron, resistivity 10 Ω cm). Before deposition, the surfaces of the substrate were sand blasted with Al_2O_3 particles at 4 bars for 30s, in order to get a substrate roughness similar to that of the foreseen application, and then cleaned in ethanol and acetone in an ultrasonic bath during 10 minutes each. The arithmetic roughness after preparation is around 4µm.

2.2 | Suspension preparation

Iodine solutions at 0, 0.1, 0.2, 0.3, 0.5, and 0.8 g/L were prepared in isopropanol and magnetically stirred for 30 minutes until complete dissolution of iodine. $Yb_2Si_2O_7$ powders were added with a concentration $[Yb_2Si_2O_7] = 30$ g/L, then exposed to ultrasonic stirring (Transsonic TI-H-15 35/130 kHz) for 15 minutes and then magnetically stirred for 12 hours. Finally, just before deposition the suspension was placed in the ultrasonic bath for 15 minutes.

2.3 | Electrophoretic process

Electrophoretic deposition for all specimens was performed using a two-cell electrode; a plate of platinum with an area of 10 cm^2 was used as anode. The silicon substrate was used as the cathode (area of 4 cm^2) at a distance of 20mm from the anode. The EPD process was performed at different voltages ($V_{app} = 50, 100, 150,$ and 200 V) and times ($t_d = 15, 30, 60, 120, 180, 300,$ and 600 seconds) using a DC power supply (sourcemeter Keithley 2611A). The current density (i) was measured during the deposition process using a computer connected to the sourcemeter (TLS express software). After

deposition, the cathode was taken off the bath at a controlled withdrawal speed of 20 mm/min. The wet coatings were dried at room temperature during 1 hour. Then the coatings were heat treated at 1300°C during 10 hours in air.

The effective voltage V_{eff} and electrical resistance of the deposit R_d at any time t were calculated using the following equations:

$$R_d(t) = \frac{V_{app}}{i(t)} - R_s, \tag{3}$$

$$V_{eff}(t) = V_{app}(t) - V_{drop}(t) \quad \text{with} \quad V_{drop} = i(t) \times R_d(t), \tag{4}$$

where V_{app} is the applied voltage and $i(t)$ is the transmitted current from electrophoretic circuit. R_s is the suspension resistance, determined using the Ohm's law by dividing the applied voltage by the current passes through the circuit at $t_d = 0$ seconds. As confirmed by conductivity measurements before and after deposition, the suspension resistance was considered as constant during the whole deposition duration (for $[I_2] = 0$ g/L $\sigma = 0.230$ μS/cm before deposition, and $\sigma = 0.236$ μS/cm after deposition). V_{app} is the applied electric voltage (constant in this study) and $V_{drop}(t)$ is the voltage drop over the deposit. R_s and R_{dep}, the resistance of the suspension and of the deposit produced by EPD are composed of two components, one resistance related to the powder and another to the interparticle liquid. Then as the current is carried by both free ions and charged particles,[27] the electrical resistance of the suspension can be obtained by the following equation:[28]

$$R_{sus} = \left[\frac{1}{R_{l,sus}} + \frac{1}{R_{p,sus}} \right]^{-1}, \tag{5}$$

where

$$R_{l,sus} = \frac{L-d}{\sigma_{l,sus}A} \tag{6}$$

and

$$R_{p,sus} = \frac{L-d}{\mu A c Q_{eff}}, \tag{7}$$

$R_{l,sus}$ represents the resistance of the ions in the suspension, $R_{p,sus}$ the resistance of the powder particles in suspension, L and A are the electrode distance (m) and surface area (m²) respectively, d is the deposit thickness (m), Q_{eff} the effective powder charge (C/kg), and $\sigma_{l,sus}$ is the conductivity of the liquid in suspension (S/m).

The deposition resistance can be calculated as follows:[28]

$$R_{dep} = \left[\frac{1}{R_{l,dep}} + \frac{1}{R_{p,dep}} \right]^{-1}, \tag{8}$$

where

$$R_{l,dep} = \frac{d}{\sigma_{l,dep}A(1-p)}, \tag{9}$$

and

$$R_{p,dep} = \frac{d}{\sigma_{p,dep}Ap}, \tag{10}$$

with $R_{p,dep}$ the resistance of the powder contribution, $R_{l,dep}$ the resistance of the liquid contribution, $\sigma_{p,dep}$ the conductivity of the dry powder in the deposit, and p is packing factor. $\sigma_{l,dep}$, the conductivity of the interparticles liquid is slightly higher than the one of the suspension $\sigma_{l,sus}$, due to counter-ions release from the particles cloud at the electrode.[28]

The mass w_d of the coatings was determined by weighting the silicon substrate before and after deposition (Atilon, $d = 0.1$ mg, max 120 g). Hence the green density $\rho_{green\ d}$ of the deposit is calculated by a mass and volume method:

$$\rho_{greend} = \frac{w_d}{S \times d} \tag{11}$$

where d is the thickness of the green deposit, and S is the deposit area.

2.4 | Suspension and coating characterizations

The zeta potential, the electrophoretic mobility, and the particle size in the suspension were measured using particle and zeta potential analyser (Zetasizer nano; Malvern). The suspension operational pH was measured using a normalized cell (WTW Inolab 7110). The electrical conductivity of the suspensions was measured as a function of $[I_2]$ with a conductimeter (Mettler Toledo, Seven2Go Cond meter S7). The XRD pattern was obtained with the diffractometer RX D4—BRUKER-AXS. Surface morphology and microstructure were investigated by scanning electron microscopy (FEG-SEM, FEI Quanta 250). Thickness of deposits was determined by step profiling using an interferometric and confocal microscope (S-Neox; Sensofar). The method consists in measuring the path difference between the coated and uncoated part of the substrate. The measurements are carried out over the length of the coating, three times in three places, in order to have a consistent average of the thickness of the coating. The results are reproducible to ±4%. The porosities of the sintered coatings are determined by image analysis (ImageJ), with five images in each case.

3 | RESULTS AND DISCUSSION

3.1 | Morphology of the Yb₂Si₂O₇ powder

The XRD diagram of the as-received $Yb_2Si_2O_7$ powder is shown in Figure 1C. All peaks correspond to the $Yb_2Si_2O_7$

phase (JCPDS 01-072-064). Figure 1 A exhibits SEM image of the powder. The particles have regular shapes with relatively uniform size (average size of 0.2 μm) which is in good agreement with granulometry measurements (Figure 1B) and the supplier specifications: $d_{50} = 300$ nm. The specific surface area was evaluated at 7 m²/g using the therory of Brunauer, Emmett and Teller method.

3.2 | Conductivity and zeta potential measurements of the suspension

Iodine is a well-known electrostatic dispersant in different organic solvents, such as acetone,[29-31] acetylacetone,[32] methanol,[33] ethanol,[29-30] and isopropanol.[34-35] The effect of iodine addition in the isopropanol solvent on both the electrical conductivity and the operational pH of the suspensions is shown in Figure 2A. The electrical conductivity linearly increases from 0.2 to 6.7 μS/cm with the iodine concentration, while the operational pH decreases from 6 to 2.5 between 0 and 1 g/L of iodine. This result suggests that free protons were formed because of a reaction between the solvent and iodine. The proton generation from iodine and isopropanol reaction is described as follows:[34-35]

$$(CH_3)_2-CH-OH+I_2 \rightleftharpoons I(CH_3)_2-COH+H^++I^-. \quad (12)$$

The concentration of H^+ increases with iodine content and causes a reduced pH value. The linear increase in the conductivity of the suspension is attributed to the formation of the free ions. Shedbakar and Bhat studied the interaction between iodine and polar solvent such as methanol and ethanol.[36-37] Based on its dielectric constant. isopropyl alcohol can also be associated to this study.

It is proved that in many donor-iodine accepter systems, the formation of triodide ions is often noticed as the medium is polar. The increase in the observed conductivity is attributed to the transformation of the initially formed 1:1 outer complex into the inner complex, followed by the fast reaction of the inner complex with iodine to form triiodide ions:[37]
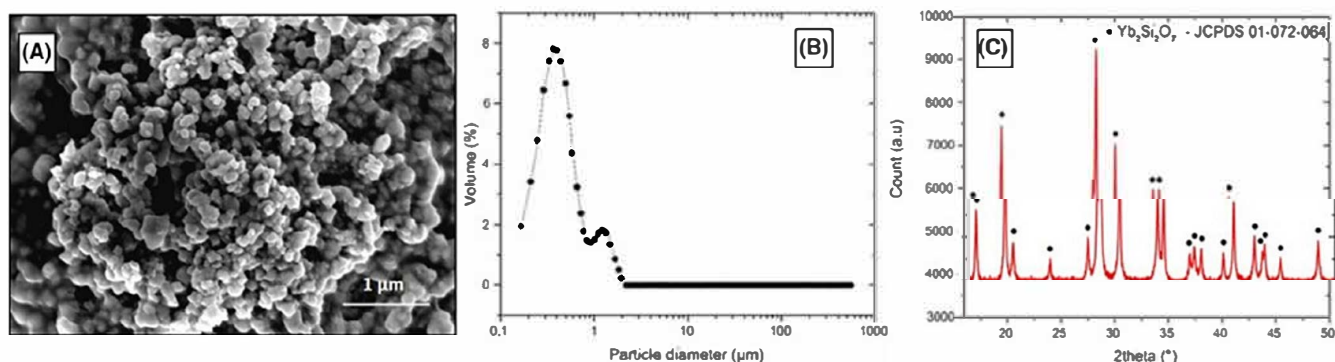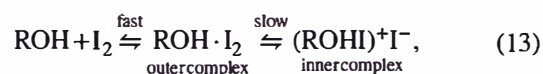
$$ROH+I_2 \overset{fast}{\underset{outercomplex}{\rightleftharpoons}} ROH \cdot I_2 \overset{slow}{\underset{innercomplex}{\rightleftharpoons}} (ROHI)^+I^-, \quad (13)$$

FIGURE 1 A, Scanning electron microscopy images, (B) size distribution of $Yb_2Si_2O_7$, and (C) XRD pattern of $Yb_2Si_2O_7$ powder [Color figure can be viewed at wileyonlinelibrary.com]
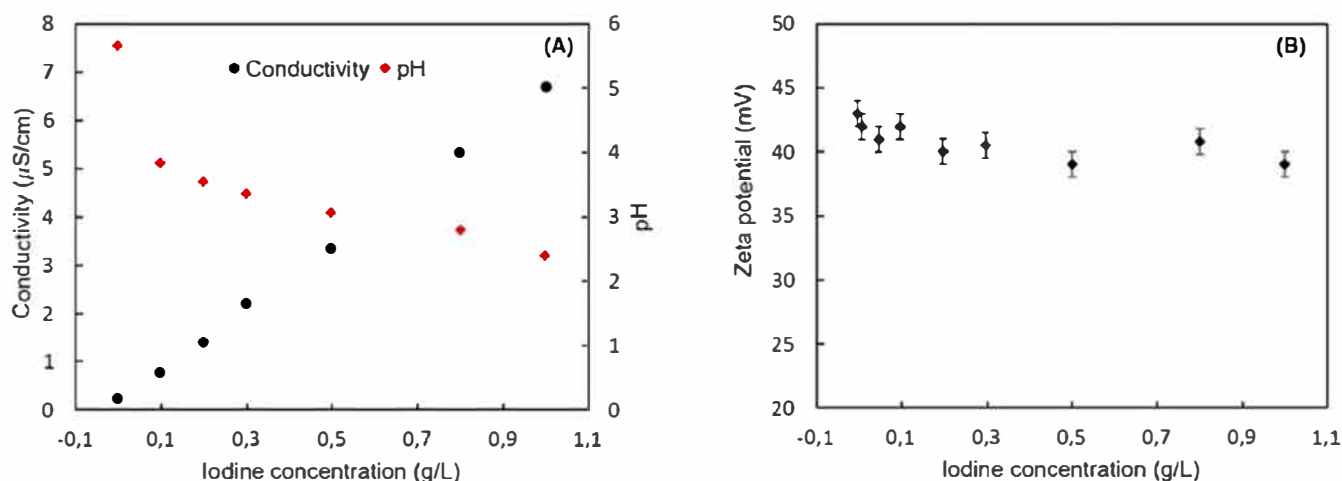

FIGURE 2 A, Effects of I_2 addition on electrical conductivity and pH on $Yb_2Si_2O_7$ isopropanol suspension, and (B) the zeta potential versus iodine concentration [Color figure can be viewed at wileyonlinelibrary.com]

$$I^- + I_2 \rightleftharpoons I^{3-}. \tag{14}$$

Another study also proved, in the case of acetone iodine solution, that surface charging mechanism takes place through the formation of $CH_3CH_2ICOH^+$ complex cations.[31] It is also suggested that, in addition to the electrostatic stabilization, the adsorption of these compounds provides a steric contribution to the stabilisation mechanism. Taking into account these elements, the formation of the complex $((CH_3)_2\text{-}CH\text{-}OHI)^+$ can be considered in this case.

The zeta potential of the ytterbium disilicate particles as a function of the iodine concentration is shown in Figure 2B. The particles acquire a positive zeta potential without iodine (+43 mV) and it remains stable around +40 mV until a concentration of 1 g/L of iodine. It means that all the suspensions are well dispersed and stable. It is usually reported that an appropriate addition of iodine in the solution enhances the adsorption of H^+ or as mentioned above the complex $(ROHI)^+$, on the surface of the particle. The adsorbed species increase the zeta potential and improve the dispersion of the colloids. In this case the zeta potential measurement shows that ytterbium disilicate particles are positively charged in pure isopropanol (Figure 2B) which suggests that the ytterbium disilicate particle surface can adsorb hydroxyl groups from moisture in air or residual water in isopropanol. The zeta potential tends to slightly decrease with increasing iodine concentration, due to the increase in the ionic strength of the suspension. This causes the compression of the double layer at high protons concentration, and consequently a decrease of the zeta potential.[16] Finally, in this case, iodine main purpose is to increase the electrical conductivity of the suspension whereas the zeta potential is not affected.

3.3 | Deposited mass and morphology of the deposit

The Figure 3 exhibits the evolution of the current density during deposition (3A), resistance of the deposit calculated with Equation 3 (3B), and electric field calculated with equation 4 divided by the inter-electrode distance (3D) as a function of time, for deposition under the constant applied voltage of 100 V, for different suspensions containing various iodine concentrations; as well as deposited mass (3C), and the suspension resistance (3E) depending on the iodine concentration. The suspensions containing iodine show a decrease in current density with deposition time reaching a plateau after maximum 200 seconds. The current densities decrease with deposition time; this is due to the formation of a deposit on the substrate with a higher electrical resistivity than the suspension one. As the iodine concentration increases, the initial value ($t = 0$) of the current density becomes higher as expected from the increase in electrical

conductivity of the suspension with iodine concentration (Figure 2A). It reaches the maximum value of 0.5 mA/cm^2 for $[I_2] = 0.8$ g/L. By increasing $[I_2]$, the slope of reduction of the current density with time increases significantly. This could be also related to the increase of the electrical conductivity of the suspension.[38]

The deposited mass increases with the iodine concentration for low iodine concentration, reaching a maximum value of 26 mg/cm^2 after 600 seconds for $[I_2] = 0.2$ g/L, and then decreases sharply. Such a behaviour could be due to the increase of ionic concentration with the increase of iodine. As mentioned previously, the ytterbium disilicate nanoparticles have a relatively high zeta potential in the suspension (Figure 2B) implying that a relatively high concentration of ions is attached to them and so in the deposit. Ytterbium disilicate acquires strongly bonded protons at its surface, whereas when iodine is added, $(ROHI)^+$ complex are formed and are weakly adsorbed on the surface. This result implies in the case of deposits from suspensions with iodine, some of the positively charged ions can be detached from the particles and migrate toward the cathode and transport the current. This suggests an increase of charge carriers in the interparticle liquid which increases its conductivity. In conclusion, it leads to the reduction of the electric resistance of the deposit (Equation 9). To explain the presence of the maximum, it should be noticed that the lower the iodine concentration, the higher the electrical resistance of the coating (for a given deposition time) (see Figure 3B), leading to a lower deposited mass. This behavior is predominant for $[I_2] < 0.2$ g/L. At higher iodine concentrations, despite a lower resistance of the deposits compared to the ones without iodine, the relatively high concentration of unabsorbed species in the suspension leads to an increase in the number of ionic species transported as compared to $Yb_2Si_2O_7$ particles. Consequently, at a deposition time of 600 seconds, whereas the electrical resistance of the coating deposited without iodine is six times higher (6 MΩ cm^2) than the one of the coating deposited with $[I_2] = 0.8$ g/L (1 MΩ cm^2), the deposited masses are very similar, around 17 mg/cm^2. Another remark concerns the deposit resistance, in the case where there is no I_2: its value is high even after only few seconds of deposition, which means that even with a small amount of coating, the deposit is highly resistive, due to the low conductivity of the liquid in the deposit.

Figure 4 compares SEM images of the surface of coatings deposited under 100 V during 3 minutes, using suspensions containing (a) $[I_2] = 0$ g/L; (b) $[I_2] = 0.1$ g/L; (c) $[I_2] = 0.3$ g/L; and (d) $[I_2] = 0.8$ g/L. The deposited coatings using suspension with low iodine contents ($[I_2] = 0$ g/L and $[I_2] = 0.1$ g/L) present a uniform microstructure with fine particles. From $[I_2] = 0.3$ g/L, agglomerates appear on the surface, but the microstructure remains dense with fine particles. At higher iodine concentration ($[I_2] = 0.8$ g/L) a rougher surface with coarse agglomerates, and a porous microstructure
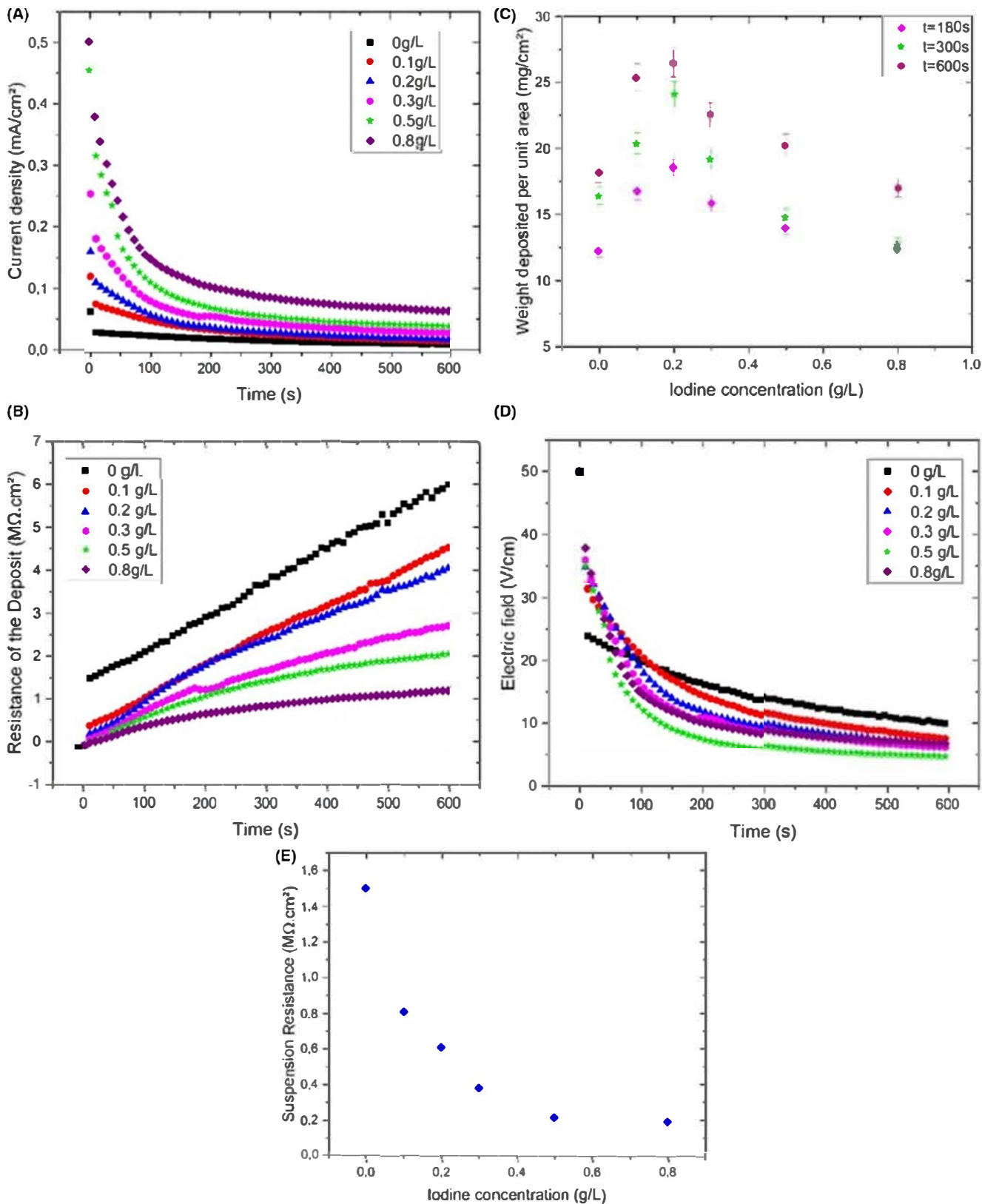
FIGURE 3 A, Current density, (B) deposit resistance (C) variations in deposit weight as a function of iodine concentration for different times and (D) electric field measured during deposition, for different iodine concentrations as a function of time ($V_{app} = 100$ V), and (E) the resistance of the suspension measured of iodine concentration determined using the Ohm's law by dividing the applied voltage by the current through the circuit at $t_d = 0$ s [Color figure can be viewed at wileyonlinelibrary.com]
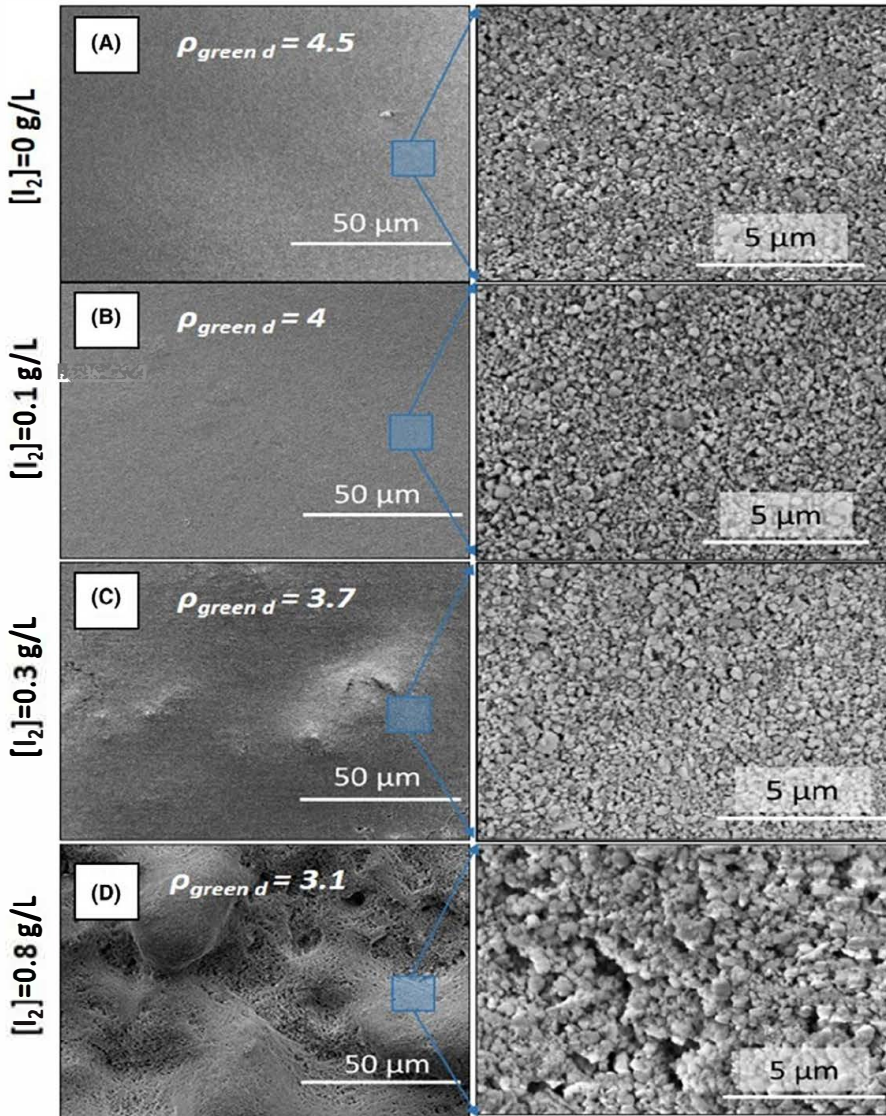
FIGURE 4 Scanning electron microscopy images of the $Yb_2Si_2O_7$ coatings deposited at $U = 100$ V from the suspension containing (A) $[I_2] = 0$ g/L, (B) $[I_2] = 0.1$ g/L, (C) $[I_2] = 0.3$ g/L, and (D) $[I_2] = 0.8$ g/L, respectively [Color figure can be viewed at wileyonlinelibrary.com]

is obtained. It can be noticed that the measured green density decreases with the iodine concentration, going from 4.5 g/cm^3 for the coating produced without iodine to 3.1 g/cm^3 with $[I_2] = 0.8$ g/L. The density of ytterbium disilicate is equal to 6.13.[7] The green density could also be correlated to the packing factor p (Equations 9 and 10), which is a parameter influencing the electrical resistance of the final coating.

As expected, the electrical resistance of the deposit increases with the deposition time, due to the increase in the deposit thickness (d parameter in Equations 9 and 10). As the resistivity of the dry ytterbium disilicate powder is very high, the deposit resistance R_{dep} is nearly equal to the resistance of interparticles liquid in the deposit ($R_{l,dep}$).

$$R_{dep} \approx R_{l,dep} = \frac{d}{\sigma_{l,dep}A(1-p)}. \tag{15}$$

With $\sigma_{l,dep}$, the conductivity of the interparticles liquid, which is slightly higher than the suspension conductivity,

due to the containment of ions at the vicinity of the electrode.[24] As it is shown previously (Figure 3B), the lower the iodine concentration, the higher the electrical resistance of the coating (for a given deposition time). So, considering the Equation (13), with a surface area A identical for the coatings, and the rather similar thickness d of the deposited coatings at 100 V after 600 seconds (42 μm for $[I_2] = 0$ g/L and 50 μm for $[I_2] = 0.8$ g/L), the packing factor and the conductivity of the interparticles liquid in the coating remain the more critical parameters on the electrical resistance. As it is proved previously, the packing factor decreases with the iodine concentration, whereas the conductivity increases, leading to the decrease in the electrical resistance.

3.4 | Kinetics of deposition

Figure 5 shows the deposition weight of $Yb_2Si_2O_7$ vs time depending on the iodine concentration ($[I_2] = 0$-0, 1-0,

2-0, 8 g/L). According to Hamaker's relation, the deposited weight increases as both deposition time t and applied voltage V_{app} increase. However, in all cases, two distinct regions can be pointed. In the first one, for $t < 120$ seconds, the evolution is linear while as expected for long deposition times ($t > 120$ seconds), the real deposited mass deviates from Hamaker's law. A plateau in deposited mass is reached around $t = 600$ seconds for all compositions. The depletion of particles from the suspension can slow down the deposition.[22] However, the relatively loaded suspensions used in this work, showed that by using them repeatedly (up to eight times), there was no significant change in the mass deposited at the elec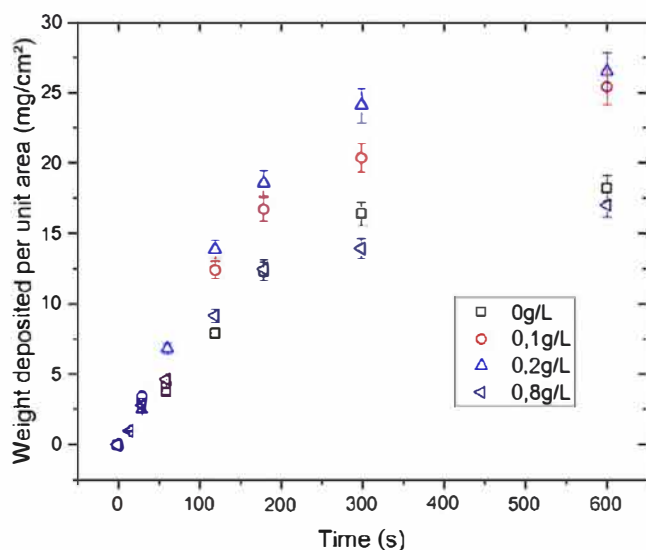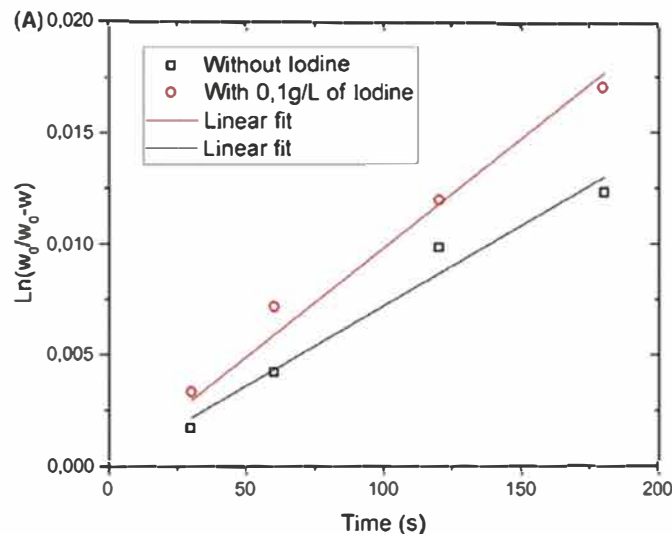trode. In this case, the decrease of the electric field is mainly responsible for the deposition rate's reduction. Indeed, as it is shown in Figure 4D, the electric field at $t = 600$ seconds is equal to 19 V/cm for $[I_2] = 0$ g/L and 6 V/cm for $[I_2] = 0.5$ g/L while the initial electric field is around 50 V/cm.

According to Zhang,[39] the changes in weight of deposited coatings over time could be represented by a parabolic equation according to the following ones (represented in Figure 6A):

$$w_t = w_0(1 - e^{-t_d/\tau}) \quad (16)$$

with w_0 the initial weight of particles in the suspension, t_d the deposition time and τ a kinetic constant which could be calculated with the following relation[22]:

$$\tau = \frac{V}{fAE\mu_e}, \quad (17)$$

where V (cm³) is the volume of suspension, A (cm²) the deposited area, μ_e (m²/V s) the electrophoretic mobility, E (V/cm), the electric field at the deposit/suspension boundary, and f the sticking factor. Not all the particles of $Yb_2Si_2O_7$ which move toward the substrate electrode during EPD, are deposited on the substrate. The f factor, also called sticking factor represents the fraction of deposited to suspended particles. According to the Equations (16) and (17), the f factor can be calculated. It is presented in Figure 6B as a function of time. The sticking factor is calculated for two suspensions with $[I_2] = 0$ and 0.1 g/L, taking into account the suspension volume (100 mL), the applied voltage (100 V) and the electrophoretic mobility (0.35 µm cm/V s). The value of the sticking factor decreases with the deposition time. It could be related to the growth of the electrically resistant layer on the surface electrode.[40] The reduction is more
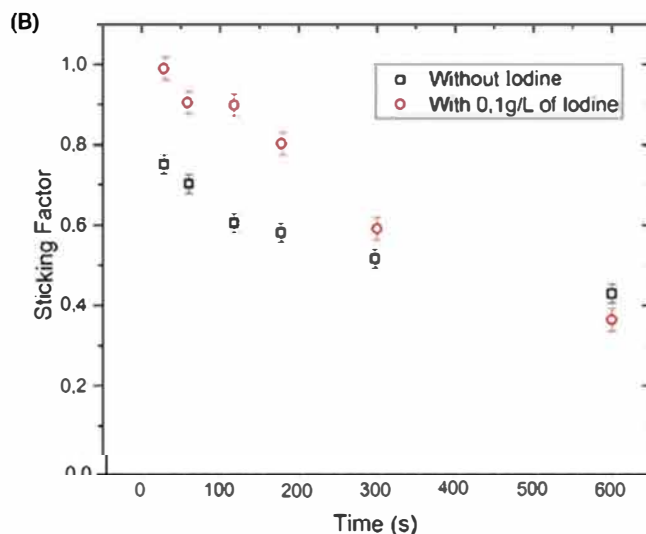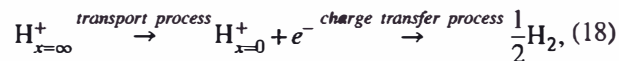

FIGURE 5 Variation in deposited weight per unit area as a function of time for $[I_2] = 0$-0.1-0.2 and 0.8 g/L at $V_{app} = 100$ V [Color figure can be viewed at wileyonlinelibrary.com]

FIGURE 6 Variation in deposited weight of $Yb_2Si_2O_7$ (A), and calculated values for sticking factor f (Equation 15), (B), as a function of deposition time for and applied voltage of 100 V, for two suspensions: without iodine and containing $[I_2] = 0.1$ g/L [Color figure can be viewed at wileyonlinelibrary.com]

important for $[I_2] = 0.1$ g/L than without iodine, following the trend of the decrease of the effective electric field (Figure 3D). Until 180 seconds of deposition time, the f factor is lower for the suspension without iodine, than the one with 0.1 g/L; this is due to the growth of the electrically resistant layer on the surface substrate which is higher for the coating without iodine.

3.5 | Coatings morphology evolution with deposition time

The SEM cross sections of the deposited coatings of $Yb_2Si_2O_7$, for $[I_2] = 0, 0.3$, and 0.8 g/L, after 180 and 600 seconds of deposition, are gathered in Figure 7. It can be seen on Figure 7C,E, a porous zone in the vicinity of the substrate, and a uniform coating without iodine. As discussed in the previous sections, this could be generated by the ions present in the suspension, with the charged $Yb_2Si_2O_7$ particles. As

the iodine concentration increases, so does the unabsorbed ions concentration, as well as the porous zone near the substrate. Another phenomenon could be responsible of the pores near the substrate: the production of hydrogen bubbles as a result of proton reduction at the cathode, as suggested by the following equation:[41]

$$H^+_{x=\infty} \xrightarrow{transport\ process} H^+_{x=0} + e^- \xrightarrow{charge\ transfer\ process} \frac{1}{2}H_2, \quad (18)$$

where the subscript $x = 0$ corresponds to the position of the outer Helmholtz plane. The transport of protons from the bulk ($x = \infty$) to the electrode-solution interface ($x = 0$) as well as the charge transfer process involve an activation energy. If the charge transfer is at virtual equilibrium, the process is controlled by the diffusion rate of protons from the bulk to the electrode. However, no gas evolution was observed during the EPD. This is confirmed by the decrease of the deposit resistance. Indeed,
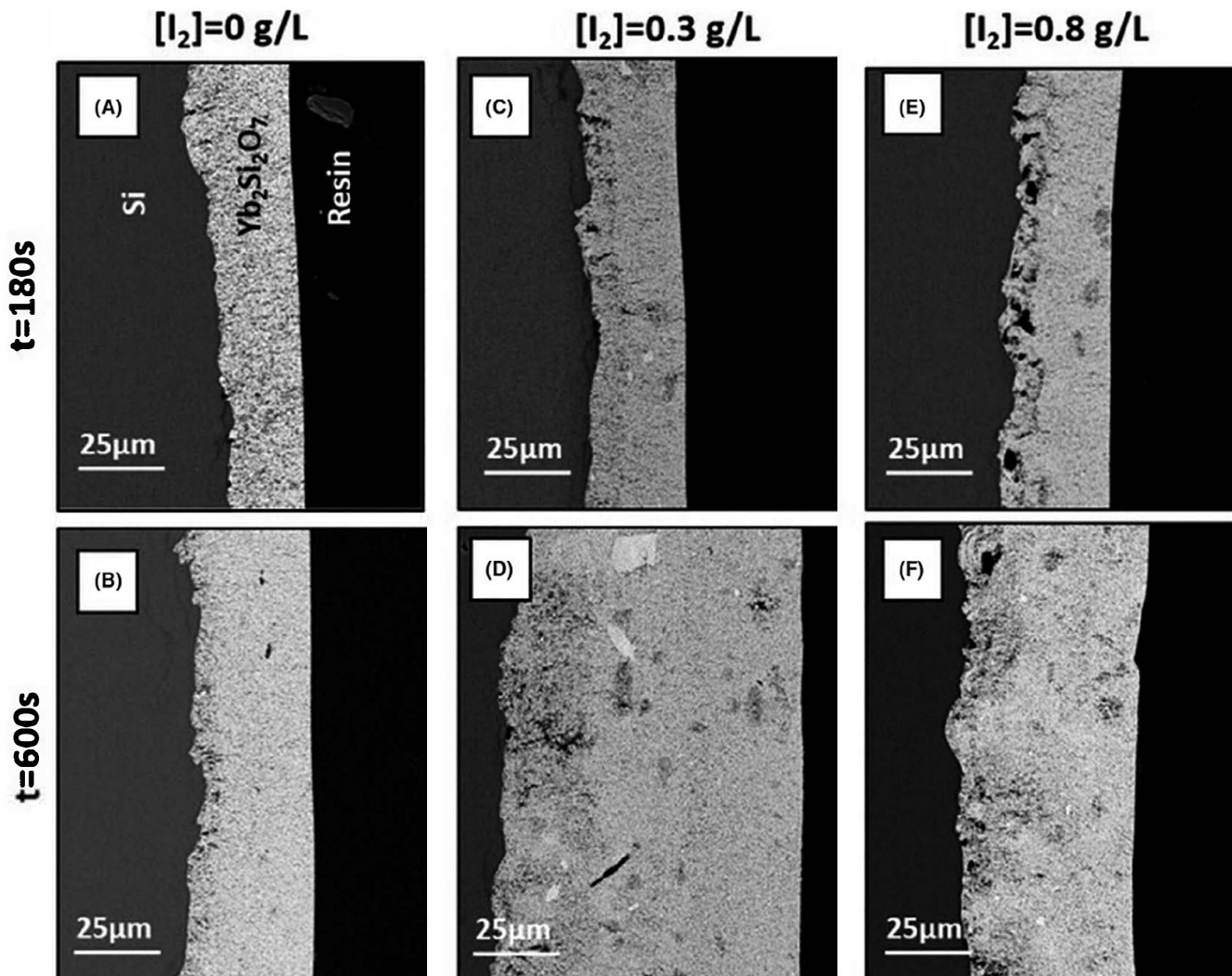

FIGURE 7 Scanning electron microscopy cross-section of $Yb_2Si_2O_7$ coating deposited at 100 V for (A, C, E) 180 s and (B, D, F) 600 s from suspension containing isopropanol media and (A, B) $[I_2] = 0$ g/L, (C, D) $[I_2] = 0.3$ g/L and (E, F) $[I_2] = 0.8$ g/L, after heat treatment at 1300°C

in the case of ion depletion at the electrode, the coating resistance should increase significantly.

On the second part of Figure 7B,D,F, the influence of the deposition time on the coating microstructure is underlined. In addition to the fact that the coating thickness is greater at 600s, especially for $[I_2] = 0.1$-0.3 g/L (30 μm without iodine, 77 μm for $[I_2] = 0.1$-0.3 g/L, and 34 μm $[I_2] = 0.8$ g/L, respectively), which is explained previously, deposits are denser. This is both confirmed by the green density of the coating at 600 seconds: 5.2, 3.9, and 3.5 g/cm^3 against 4.5, 3.7, and 3.1 g/cm^3 at 180 seconds (Figure 4), respectively, and by the global density after sintering. This is related to the decrease in the deposition rate, mainly due to the decrease of the electric field E_{eff} (Figure 3D). The coating formed without iodine is 20% denser at $t_d = 600$ seconds than at $t_d = 180$ seconds. Coatings formed with iodine are about 10% denser at $t_d = 600$ seconds. This is related to free ions present who settle in the interparticles liquid and cause more heterogeneities.

Finally, adding iodine in isopropanol suspension allows to increase the deposition rate of ytterbium disilicate powder, as long as it does not exceed 0.3 g/L. Over this value the microstructure is more affected. In the case where both a dense and thick coating is sought, the best compromise between deposition rate and dense microstructure seems to be a suspension with 0.1 g/L of iodine (not too low to keep a suitable deposition kinetics and not too high to avoid porous microstructures). It allows coatings to be thicker than those from a suspension without iodine (Figure 3C), while retaining a relatively high density (Figure 4).

3.6 | Influence of applied voltage on green density of the coatings

Figure 8 shows the deposited weight per unit area as a function of the applied voltage V_{app} for suspensions with $[I_2] = 0$ g/L and $[I_2] = 0.1$ g/L for $t = 180$ seconds. As expected, for both suspensions, the deposited mass increases with the applied voltage. The green density of the coatings is calculated as mentioned in the section "2.4 Suspension and coatings characterizations" and is reported on Figure 9. The green density decreases with the applied voltage for the coating deposited from the suspension with $[I_2] = 0.1$ g/L. This is due to the excessive motion of particles, at high applied voltage, which does not allow a good arrangement of the deposit. Negishi et al[42] have shown that the current density becomes unstable as the applied electric field increases, mostly above 50 V/cm. On the contrary, in the case of the iodine-free deposit, the green density at 50 V (3.7 g/cm^3) is still lower than the one at 100 V (4.4 g/cm^3). This result involves that, when the motion of the particles is to low, the deposit exhibits more porosities. The energy transmitted to the particles is not sufficient in the case where 50 V is applied. So that, the applied voltage

of 100 V seems the most suitable value to obtain the denser coatings. Also, it can be deduced from Figure 9 that the green density of the coating deposited with $[I_2] = 0.1$ g/L is lower than the one of the coating deposited without iodine. It can be related to the free ions concentration which is higher in the case of $[I_2] = 0.1$ g/L; they migrate toward the cathode and generate porosity.

Finally, taking into account all these coupled parameters, Figure 10 exhibits cross-sections of the deposited coatings from suspension with $[I_2] = 0$ g/L and $[I_2] = 0.1$ g/L at applied
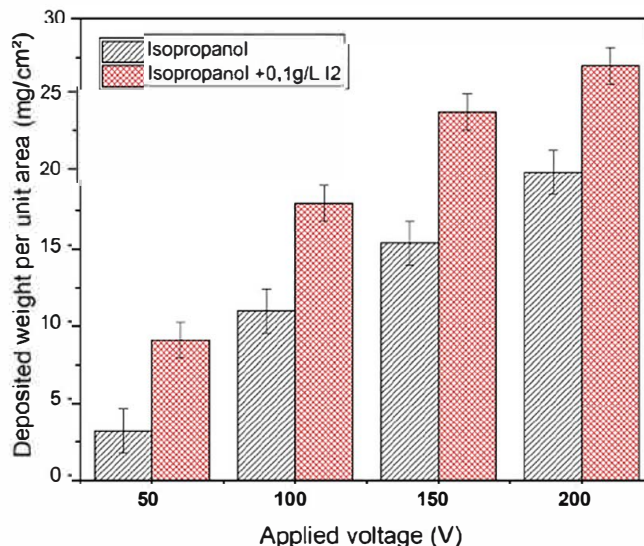

FIGURE 8 Deposited weight as a function of the applied voltage for suspension containing isopropanol and $[I_2] = 0$ g/L and $[I_2] = 0.1$ g/L after 180 s of deposition [Color figure can be viewed at wileyonlinelibrary.com]
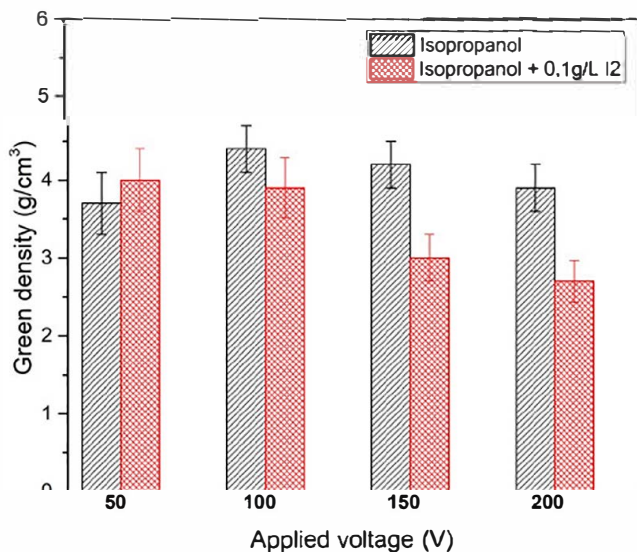

FIGURE 9 Green density of the coating as a function of the applied voltage for suspension containing isopropanol and $[I_2] = 0$ g/L and $[I_2] = 0.1$ g/L after 180 s of deposition [Color figure can be viewed at wileyonlinelibrary.com]
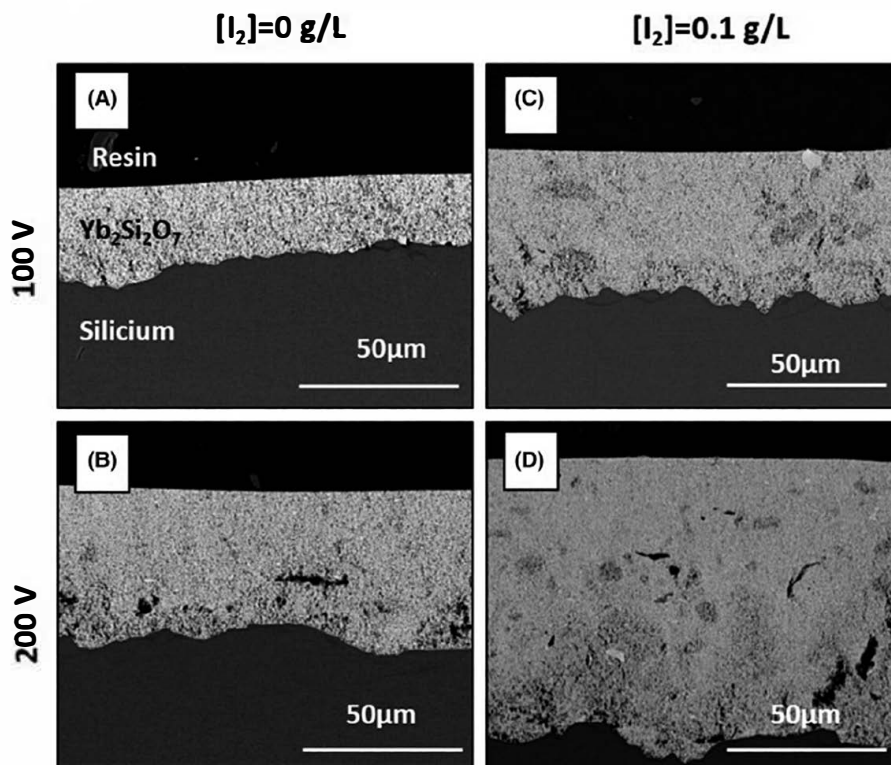
FIGURE 10 Scanning electron microscopy cross-section of $Yb_2Si_2O_7$ coatings at (A), (C) 100 V and (B), (D) 200 V, after 180 s of deposition, from suspension containing isopropanol and (A, B) $[I_2] = 0$ g/L and (C, D) $[I_2] = 0.1$ g/L, after heat treatment at 1300°C

voltage of 100 and 200 V. The effect of voltage magnitude on the coating is clearly shown in this figure. By increasing the applied voltage, the deposit microstructure becomes more porous and less uniform, due to the high velocity of the particles in higher voltage. Indeed, there is not enough time for particles to organize in the appropriate location to make the deposit denser. This result is in good correlation with the results of the Figure 9. The denser and very conformal coating was obtained with the suspension without iodine at an applied voltage of 100 V.

4 | CONCLUSION

Ytterbium disilicate coatings were deposited on silicon substrate by EPD using iodine and isopropanol as additive and solvent, respectively. All suspensions prepared with various iodine concentrations, presented high stability ($\xi = +40$ mV). It was proved that iodine acts as an effective generator of free ions, leading to the increase of the suspension conductivity. It was found that the maximum deposition rate was obtained from the suspension with 0.2 g/L. This concentration corresponds to the balance between a moderate conductivity and a low concentration of free ions in the suspension. It was observed that the coating microstructure becomes porous at high iodine concentration, because of the increase of free ions in suspension. Mass of deposited coatings increases with both increasing time and applied voltage. Relative to the microstructure, it was proved that inhomogeneities increase with the increase of applied voltage, mainly due to the high velocity of particles at high voltage and a compaction occurs when the deposition time increases because of the decrease of the deposition rate due to the increase of the electrical resistance of the deposit R_d, and consequently to the decrease of the electric field E_{eff}. Furthermore, it was shown that the sticking factor decreases with the deposition time. Finally, the denser coatings (20% of porosity) were obtained with suspension without iodine, at an applied voltage of 100 V.

ORCID
Manon Prioux https://orcid.org/0000-0001-9780-1362
Sandrine Duluard https://orcid.org/0000-0002-8095-6170

REFERENCES
1. Lee KN. Protective coatings for gas turbines. In: Dennis R (Ed.), The gas turbine handbook. Cleveland: United States Department of Energy (DOE), 2006.419–436.
2. Fu HZ. Challenge and development trends of future aero engine materials. J Aeronaut Mater. 1998;18(4):52–61.
3. Opila EJ, Hann RE Jr. Paralinear oxidation of CVD SiC in water vapor. J Am Ceram Soc. 1997;80(1):197–205.
4. Opila EJ. Variation of the oxidation rate of silicon carbide with water-vapor pressure. J Am Ceram Soc. 1999;82(3):625–36.
5. Robinson RC, Smialek JL. SiC recession caused by SiO_2 scale volatility under combustion conditions. I. Experimental results and empirical model. J Am Ceram Soc. 1999;82(7):1817–25.
6. Jacobson NS, Fox DS, SmialekJL DC, Lee KN, GRC. Performance of ceramics in severe environments. Cleveland: NASA Glenn Research, 2005; p. 1–36.

7. Flesche J. Polymorphism and crystal data of the rare-earth disilicates of type R.E.2Si$_2$O$_7$. J Less Common Met. 1972;21:1–14.

8. Auger ML, Sarin VK. The development of CVD mullite coatings for high temperature corrosive applications. Surf Coat Technol. 1997;94–95:46–52.

9. Harder BJ, Zhu D. Physical vapour deposition of thermal and environmental protection system. ITSC 2012, Houston TX, May 21–24 2012.

10. Von Niessen K, Gindrat M. Plasma spray-PVD: a new thermal spary process to deposit out of the vapour phase. J Therm Spray Technol. 2011;20(4):736–43.

11. Ramasamy S, Tewari SN, Lee KN, Bhatt RT, Fox DS. Environmental durability of slurry based mullite-gadolinium silicate on silicon carbide. J Eur Ceram Soc. 2011;31:1123–30.

12. Al Nasiri N, Patra N, Pezoldt M, Colas J, Lee WE. Investigation of a single-layer EBC deposited on SiC/SiC CMCs: processing and corrosion behaviour in high-temperature steam. J Eur Ceram Soc. 2019;39:2703–11.

13. Van der Biest O, Vandeperre L, Put S, Anné G, Vleugels J. Laminated and functionally graded ceramics by electrophoretic deposition. Adv Sci Technol. 2006;45:1075–84.

14. Abdoli H, Zarabian M, Alizadeh P, Sadrnezhaad SK. Fabrication of aluminium nitride coatings by electrophoretic deposition: effect of particle size on deposition and drying behaviour. Ceram Int. 2011;37(1):313–9.

15. Maleki-Ghaleha H, Rekabeslami M, Shakeri MS, Siadati M, Javidi M, Talebian S, et al. Nano-structured yttria-stabilized zirconia coating by electrophoretic deposition. App Surf Sci. 2013;280:666–72.

16. Besra L, Liu M. A review on fundamental and applications of electrophoretic deposition. Prog Mater Sci. 2007;52(1):1–61.

17. Koelmans H, Overbeek G. Stability and electrophoretic deposition of suspensions in non-aqueous media. Discuss Faraday Soc. 1954;18:52–63.

18. Zhitomirsky I. Cathodic electrodeposition of ceramic and organoceramic materials: fundamental aspects. Adv Colloid Interface Sci. 2002;97:279–317.

19. Das D, Basu RN. Suspension chemistry and electrophoretic deposition of zirconia electrolyte on conducting and non-conducting substrates. Mater Res Bull. 2013;48:3254–61.

20. Saberi F, Shayegh B, Doostmohamdi A, Baboukani AR, Asadikiya M. Electrophoretic deposition kinetics and properties of ZrO$_2$ nano coatings. Mater Chem Phys. 2018;213:444–54.

21. Farrokhi-Rad M, Shahrabi T. EPD of titania nanoparticles: sticking parameter determination. J Am Ceram Soc. 2012;95(11):3434-40.

22. Sarkar P, Nicholson PS. Electrophoretic deposition (EPD): mechanisms, kinetics, and application to ceramics. J Am Ceram Soc. 1996;79(8):1987–2002.

23. Ferrari B, Moreno R. EPD kinetics: a review. J Eur Ceram Soc. 2010;30:1069–78.

24. Van der Biest O, Vandeperre L. Electrophoretic deposition of materials. Annu Rev Mater Sci. 1999;29:327–52.

25. Hamaker HC. Formation of a deposit by electrophoresis. Trans Faraday Soc. 1940;36:279–87.

26. Smoluchowski M. Versuch einer mathematischen Theorie der Koagulationkinetik kolloider Loesungen. Z Phys Chem. 1917;92:129–32.

27. Sussman A, Ward TJ. Electrophoretic deposition of coatings from glass-isopropanol slurries. RCA Rev. 1981;42:178.

28. Van Der Biest O, Put S, Anne G, Vleugels J. Electrophoretic deposition for coatings and free standing objects. J Mater Sci. 2004;39(3):779–85.

29. Yiang K, Shen JH, Yang KY, Hung IM, Fung KZ, Wang MC. Characterization of the yttria-stabilized zirconia thin film electrophoretic deposited on La$_{0.8}$Sr$_{0.2}$MnO$_3$ substrate. J Alloy Compd. 2007;436:351–7.

30. Chen F, Liu M. Preparation of yttria-stabilized zirconia (YSZ) films on La$_{0.85}$Sr$_{0.15}$MnO$_3$ (LSM) and LSM±YSZ substrates using an electrophoretic deposition (EPD) process. J Eur Ceram Soc. 2001;21:127–34.

31. Dusoulier L, Cloots R, Vertruyen B, Moreno R, Burgos-Montes O, Ferrari B. YBa$_2$Cu$_3$O$_{7-x}$ dispersion in iodine acetone for electrophoretic deposition: surface charging mechanism in a halogenated organic media. J Eur Ceram Soc. 2011;31:1075–86.

32. Ji C, Lan W, Xiao P. Fabrication of yttria-stabilized zirconia coatings using electrophoretic deposition: packing mechanism during deposition. J Am Ceram Soc. 2008;91(4):1102–9.

33. Kadam MB, Sinha BB, Kalubarme RS, Pawar SH. Transformation of MgB$_2$ powder into superconducting film via electrophoretic deposition technique. J Alloy Compd. 2009;478:467–73.

34. Lee YH, Kuo CW, Shih CJ, Hung IM, Fung KZ, Wen SB, et al. Characterization on the electrophoretic deposition of the 8 mol% yttria-stabilized zirconia nanocrystallites prepared by a sol-gel process. Mater Sci Eng. 2007;445:347–54.

35. Jia L, Lü Z, Huang X, Liu Z, Chen K, Sha X, et al. Preparation of YSZ film by EPD and its application in SOFCs. J Alloy Compd. 2006;424:299–303.

36. Bhat SN, Dwivedi R. Transference number of charge-transfer complexes in solutions: methanol-iodine and ethanol-iodine. Proc Indian Acad Sei (Chem Sci). 1980;89(4):337–40.

37. Shedbalkar VP, Bhat SN. Transport number of charge transfer complexes in solution. Electrochim Acta. 1983;28(3):359–61.

38. Stappers L, Zhang L, Van der Biest O, Fransaer J. The effect of electrolyte conductivity on electrophoretic deposition. J Colloid Interface Sci. 2008;328:436–46.

39. Zhang Z, Huang Y, Jiang Z. Electrophoretic deposition forming of SiC-TZP composites in a non-aqueous sol media. J Am Ceram Soc. 1994;77:1946–9.

40. Kavanlouei M, Akbari A. Electrophoretic deposition of titanium nitride coatings. J Am Ceram Soc. 2019;101:3288–98.

41. Fukada Y, Nagarajan N, Mekky W, Bao Y, Kim HS, Nicholson PS. Electrophoretic deposition—mechanisms, myths and materials. J Mater Sci. 2007;39:787–801.

42. Negishi H, Yanagishita H, Yokokawa H. Proceedings of the electrochemical society on electrophoretic deposition: fundamentals and applications. 2002;2002(21:):214–21.